



HAL
open science

HARMONI ELT instrument : Integral Field Unit cryogenic engineering models results

Matthieu Guibert, Jean-Emmanuel Migniau, Magali Loupiau, Alexandre Jeanneau, Alban Remillieux, Karen Disseau, Eric Daguisé, Diane Chapuis, Didier Boudon, Nicolas Bouché, et al.

► **To cite this version:**

Matthieu Guibert, Jean-Emmanuel Migniau, Magali Loupiau, Alexandre Jeanneau, Alban Remillieux, et al.. HARMONI ELT instrument : Integral Field Unit cryogenic engineering models results. *Advances in Optical and Mechanical Technologies for Telescopes and Instrumentation V*, Jul 2022, Montréal, Canada. pp.50, 10.1117/12.2629829 . hal-04798326

HAL Id: hal-04798326

<https://hal.science/hal-04798326v1>

Submitted on 22 Nov 2024

HAL is a multi-disciplinary open access archive for the deposit and dissemination of scientific research documents, whether they are published or not. The documents may come from teaching and research institutions in France or abroad, or from public or private research centers.

L'archive ouverte pluridisciplinaire **HAL**, est destinée au dépôt et à la diffusion de documents scientifiques de niveau recherche, publiés ou non, émanant des établissements d'enseignement et de recherche français ou étrangers, des laboratoires publics ou privés.

HARMONI ELT instrument

Integral Field Unit cryogenic engineering models results

Matthieu Guibert^a, Jean Emmanuel Migniau^a, Magali Loupiau^a, Alexandre Jeanneau^a, Alban Remillieux^a, Karen Disseau^a, Eric Daguisé^a, Diane Chapuis^a, Didier Boudon^a, Nicolas Bouché^a, Johan Richard^a, Hermine Schnetler^b, Dave Melotte^b, Niranjan A. Thatte^c, Fraser Clarke^c, Matthias Tecza^c, on behalf of the HARMONI consortium.

^aUniv Lyon, Univ Lyon1, Ens de Lyon, CNRS, Centre de Recherche Astrophysique de Lyon UMR5574, F-69230, Saint Genis-Laval, France;

^bUK Astronomy Technology Centre, Royal Observatory, Edinburgh EH9 3HJ, United Kingdom;

^cUniv. Of Oxford, Keble Road, Oxford, United Kingdom;

ABSTRACT

HARMONI is the first light visible and near-IR integral field spectrograph for the ELT. It covers a large spectral range from 450nm to 2450nm with resolving powers from 3500 to 18000 and spatial sampling from 60mas to 4mas. It can operate in two Adaptive Optics modes - SCAO and LTAO - or with NOAO. The Integral Field Unit (IFU) sub-system is part of an Integral Field Spectrograph cooled down at 130K. The IFU is in charge of splitting, slicing and rearranging the rectangular field of view into 4 long slits (~540mm) to feed 4 spectrographs. It consists of more than 60 mirrors blocks that have to be aligned and maintained inside the HARMONI cryostat. As the project prepares for Final Design Reviews, we present the design of the IFU mirror mounts as well as performance results obtained on engineering models.

Keywords: Integral Field Unit

1. INTRODUCTION

The High Angular Resolution Monolithic Optical and Near-infrared Integral field spectrograph or HARMONI is a first light instrument for the ESO Extremely Large Telescope. It will provide more than 30000 spectra in one single exposure, spanning the 0.45 to 2.45 μ m range. A dedicated paper about the HARMONI instrument capabilities are presented in [1]. The light going through the ELT is corrected by an adaptive optic system and then enters a cryostat called the Integral Field Spectrograph (IFS), described in this conference article [2] and represented in Figure 1-1. The IFS is made up of 6 sub-systems. The cryostat encloses five sub-systems, and provides them an operating temperature of 130K. The light enters the cryostat into the Pre-Optics sub-system, which provides a pupil cold stop and 4 different spatial scales (4x4mas, 10x10mas, 20x20mas and 30x60mas). Then it goes through the IFU, which is responsible for dividing the field and reshaping it, to provide four output slits arranged in a square at the input of the four spectrographs. The four Infrared Spectrographs include a set of gratings to providing a spectral resolution ranging from 3000 up to 20000. All spectrographs cover the wavelength range from 0.8 to 2.45 μ m, in addition two of them have a visible path covering the wavelength range from 0.5 to 0.8 μ m. They are equipped with eight IR detectors (i.e., two by spectrograph) and four visible detectors 4k*4k (i.e., two by visible path). The cryostat is held by the sixth sub-system, the rotator wrap, which makes it rotate during the observation.

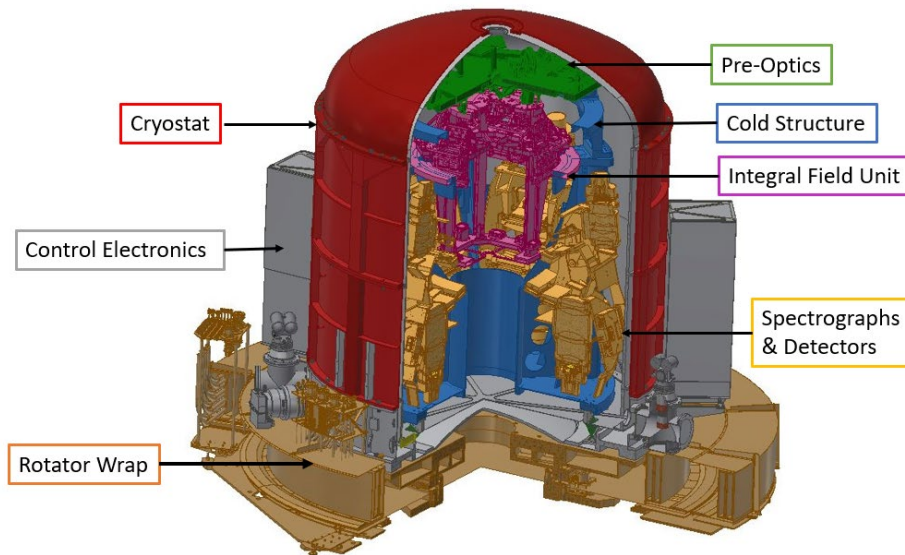


Figure 1-1 : general section of the Integral Field Spectrograph.

While the IFU design, budget and expected performances have been described in [3], a general view of this system is shown in Figure 1-2. As a reminder, this setup operates in vacuum at 130K. The Integral Field Unit is composed of two main optical modules, namely the Splitting and Relay Module (SRM) and Image Slicer Module (ISM) together with a structural module called IFU Main Structure (IMS). The input of the IFU is a rectangular field of view delivered by the IFS Pre-Optics (IPO) Sub-System. Circa 100 mirrors are composing the Integral Field Unit.

The alignment procedures of its relay mirrors and slicer mirrors is proposed to be done at warm conditions, based on a Structural-Thermal-Optical-Performance (STOP) while the overall performance of the system will be checked in cold conditions when assembled with all other sub systems of the spectrograph. In this scheme, the mirrors need to be athermal to within 10 arcsec with respect to their mount base in order to fulfill their overall tolerance of 40 arcsec. These points drove the main characteristic of our design: the ability to keep an angular position from warm to cold conditions. Therefore, the design of their mounts was qualified building different engineering models, and qualifying them in CRAL's test cryostat.

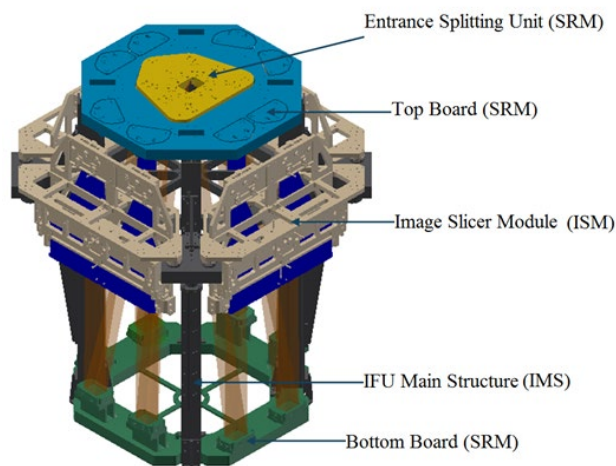


Figure 1-2 : general view of the Integral Field Unit.

The first optical and mechanical designs of mirror mount and their associated tests are described in Section 2. Section 3 describes an improved design of this first draft, and its associated tests. Section 4 describes a version of the mount where all six degrees of freedom can be tuned and blocked. Unfortunately, at the time of the writing of this article, the delivery of this last set up has been delayed due to supply chain issues at our supplier, and no tests of this set up can be presented in this paper.

2. MIRROR STATIC KINEMATIC MOUNT

2.1 Design description

This first design relies on the use of shims to set the angular position of the mirror. The mirror is glued on an Invar plate, which is positioned through a kinematic joint to an aluminium base plate. The kinematic joint is made of 2 spherical pistons acting on grooves to block the X, Y, and θZ movements. One of these grooves has a cone shape, while the other has a linear shape. These pistons are free to move along the vertical direction, and pushed on their respective groove with springs, ensuring a contact whatever the size of the shims used and compensating the thermal expansion difference between the shims and the invar plate. The θX , θZ and Z movements are blocked through 3 pins on flat contacts, which act as shims to adjust the static angular position of the mirror along these directions. This setup is represented in Figure 2-1. 4 thermal braids are connecting the base plate to the Invar plate to improve thermal conduction of the mirror. The Invar plate is maintained in contact with the pins using 4 screws associated with Belleville washers as springs.

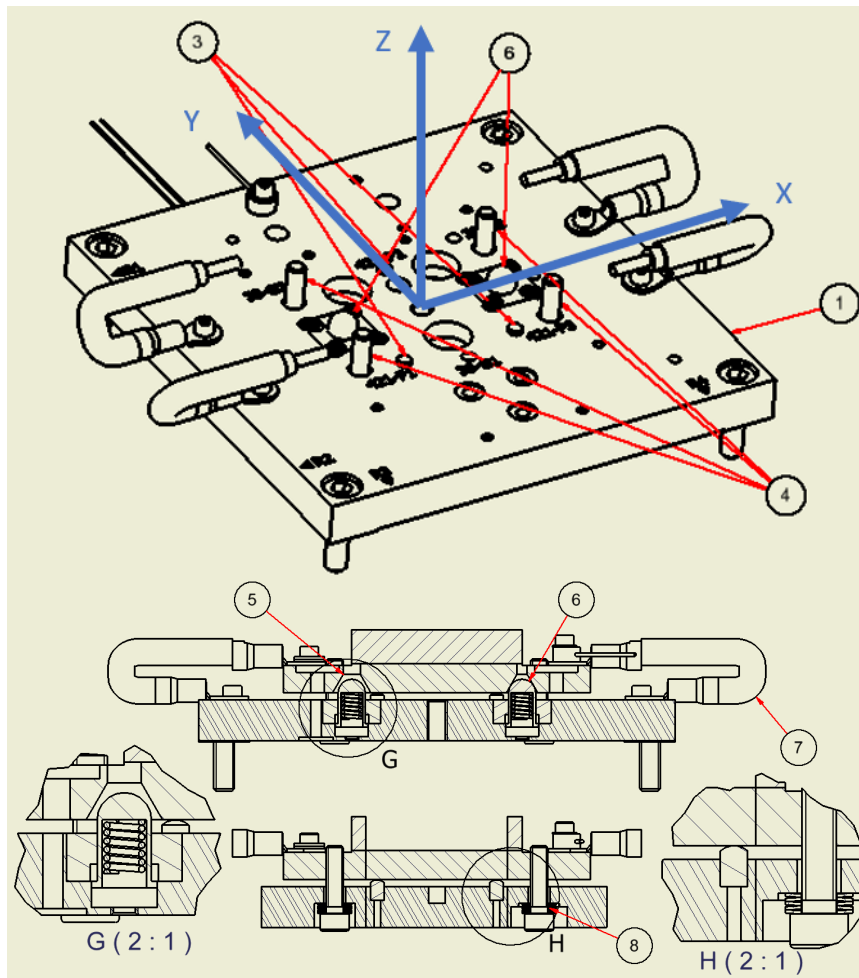


Figure 2-1 : detailed view of mirror mount : 1-base plate (aluminium), 3-mechanical shims, 4-retaining screws, 5-linear groove, 6-point groove, 7-thermal braid, 8-Belleville washers.

2.2 Flatness measurements

The proposed design implies a flexion of the Invar plate. To ensure that deflection of the plate is compliant with the expected mirror flatness specification, a FEA analysis study was carried out. Its results were compared with measurements of the mirror surface carried out with a Fizeau interferometer (Zygo verifireXPD). Both analysis and measurements agreed, as shown in Figure 2-2, and are compliant with the expected surface deformation.

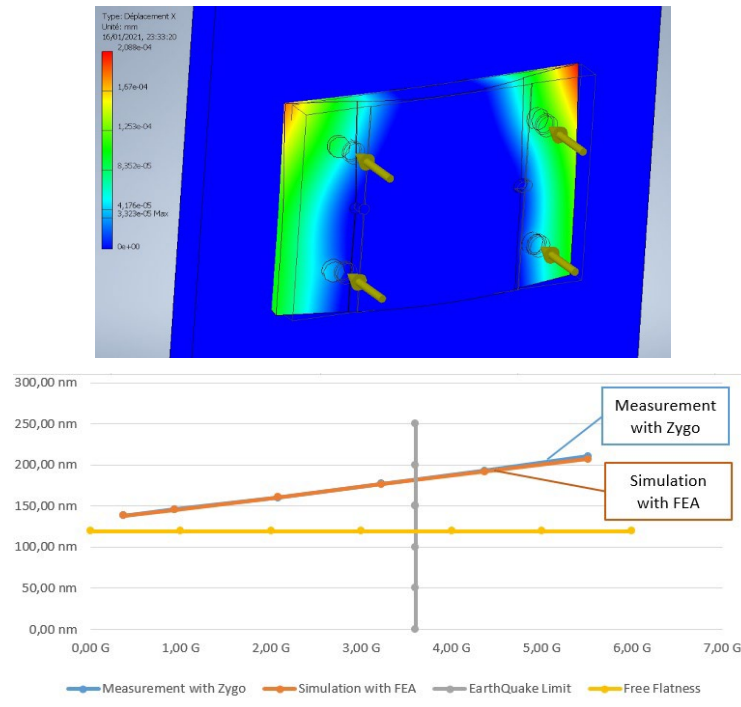


Figure 2-2 : FEA analysis versus flatness direct measurements. Retaining screws forces are expressed in G, to be compared with the 3.6G specification that the mount should handle.

2.3 Cryogenic tests

Measurements of the mirror position during cooling were carried out in a test cryostat. The engineering model was placed inside a vacuum chamber, positioned on a plate cooled by a cryomech PT90 cryocooler. A reference mirror was placed on the base plate, next to the mirror to be measured. This setup was installed in front of a viewport, in order to allow direct measurement of angular deviations of both mirrors by measuring the displacement of a reflected laser beam on a detector.

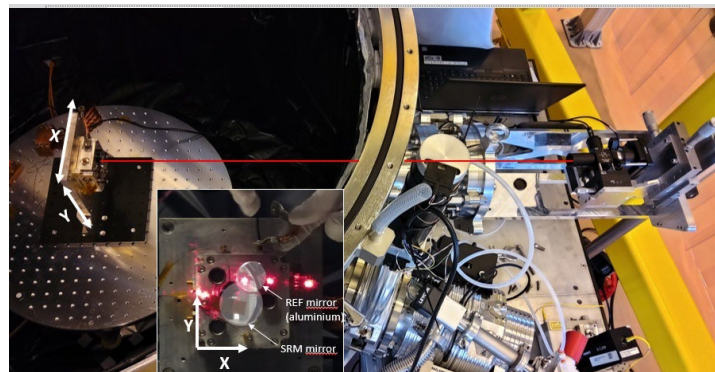


Figure 2-3 : cryogenic angular stability measurement setup

With this setup, we observed a parasitic movement of the mirror compared to the reference mirror of 80 arcsec (see Figure 2-4).

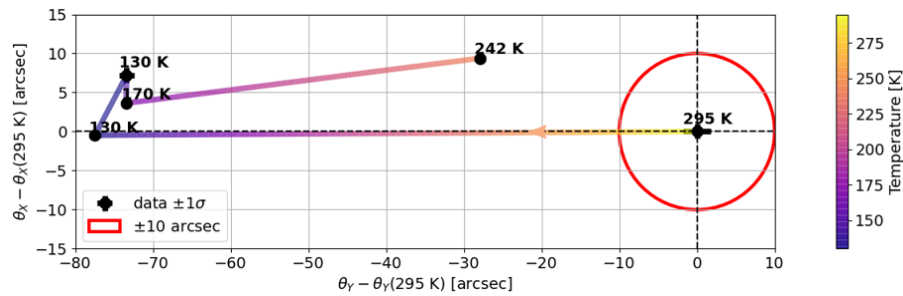


Figure 2-4 : observed angular deviation of the mirror with respect to its orientation at 295K.

Our main analysis was that the influence of the thermal braid was significant during cooling. Furthermore, the pin on flat contact present a very low local stiffness, and therefore are subject to deformation when a change in contact pressure is seen by the engineering model. Furthermore, the stability of our measurement setup for the full time of the cooling was not certain.

From these observations, decision was taken to develop a new engineering model solving these issues, and to improve our measurement set up.

3. MIRROR MOUNT ALLOWING ONLINE TETA-TETA TUNING

3.1 Design description

Two main aspects drove the development of this new engineering model: the poor angular stability results described in Section 2, but also the fact that a change of the mirror position implied to unmount completely the mirror. Therefore, uncertainty linked to the static positioning could be added to the final mirror position. In this new proposed design, shimming is replaced by in situ tuning of the mirror position.

Other limitation of the first prototype are also cancelled with the new design. The first one is flexion induced by the fact that maintaining screws and pins were not at the same position. We propose now a design where the shim function and the maintaining force are concentric on the same axis. The second one concerns the low allowable value of maintaining force limited by the sphere on plan contact of the shims. This is cancelled by the use of sphere on sphere contact. These improvements are implemented in the new pre-constrained differential screw described in Figure 3-1.

The working principal of this screw is that the 2 nuts having thread of 0.5- and 0.75-mm pitches allows us to have an apparent pitch of 0.25 mm, while allowing high internal forces in the threads of the screw. Furthermore, these 2 nuts are separated with a spring that cancelled the backlash present in the nuts. Of course, this spring limits the total stroke of our system, but this stroke does not have to be very important (ie 200 μ m) as the system is only here to correct error from the nominal position of the mirror. The Belleville washers that are located underneath the head of the screw are the one “pulling” on the Invar plate. The contact between the nut and the Invar plate is made through 2 spherical washers, allowing high forces to be transmitted. On the top of the system, a fine screw allows us to block the rotation of the screw if needed.

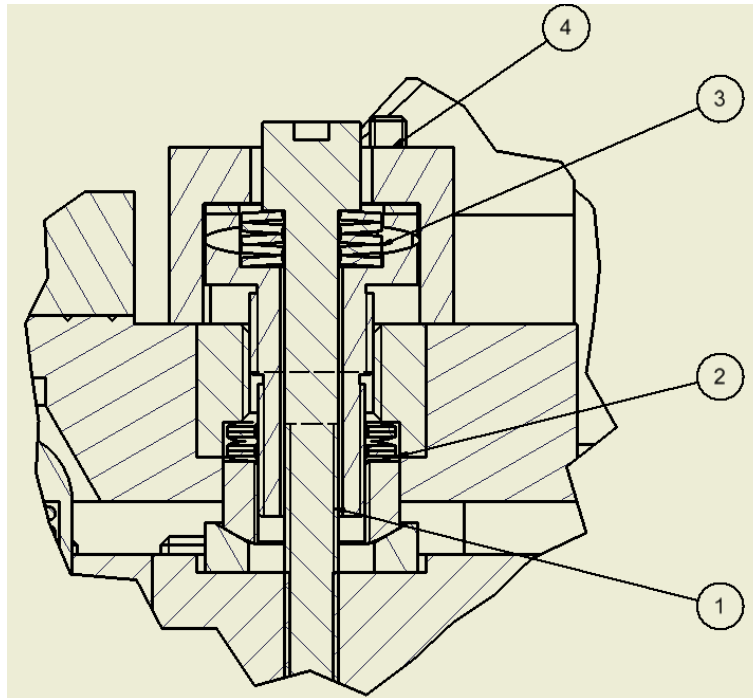


Figure 3-1 : detailed view of pre-constrained differential screw : 1-differential screw, 2- pre constrain spring, 3- retaining Belleville washers, 4-blocking screw

This screw is installed on our new engineering model as represented in Figure 3-2. 3 screws are used to ensure an isostatic mounting of the mirror.

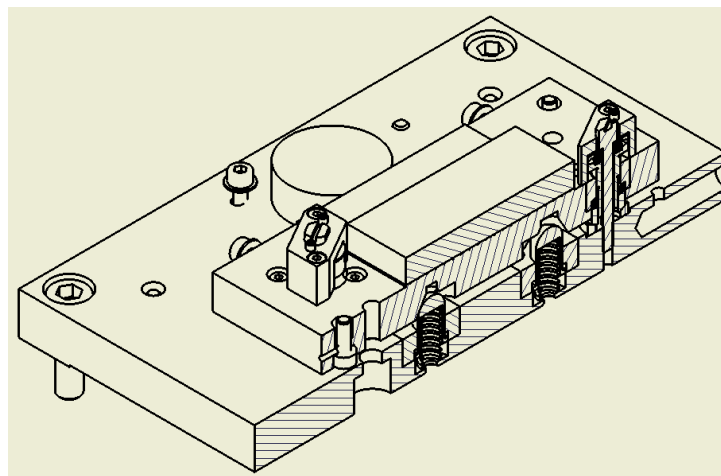


Figure 3-2 : tunable mirror mount. Shims have been replaced by pre constrain differential screws

3.2 Tuning resolution

Mounted on a single axis in front of a gage, the resolution obtained by this screw is in the order of $0.1 \mu\text{m}$. We have equipped our engineering model with a 3 numerical gages setup as represented Figure 3-4. Connected to a PC that compute the inverse kinematic of the position from the reading of the gages, we are able to tune the position screws

reading the position in live. This setup allows us to control independently the position of the Invar plate from the base plate with a resolution better than $0.1\mu\text{m}$ and few arcseconds. This capability is illustrated in the curve represented in Figure 3-3, where the 3 tunable positions are represented versus the time in seconds. On this curve, we represent the time spent to move the mirror of $20\mu\text{m}$ along the z direction, with no angular deviation. The last minute of the experiment represents the parasitic move measured when blocking screws are activated. Within a short time, the mirror is positioned at $1\mu\text{m}$ from the target position, and rotation are kept under $3''$.

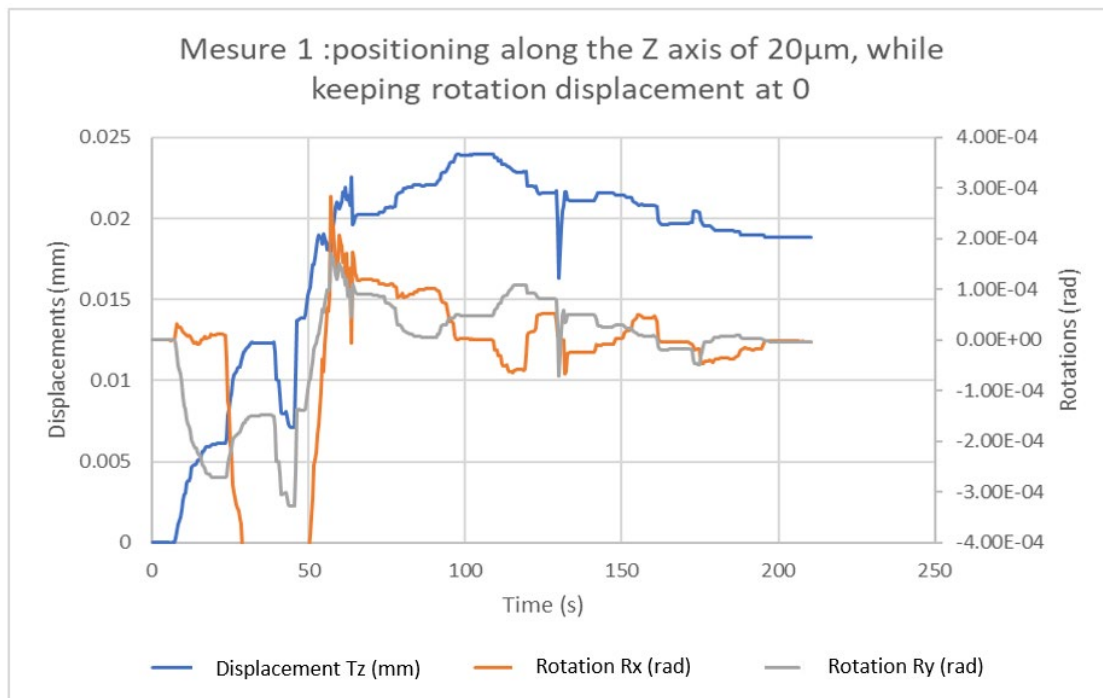


Figure 3-3 : tuned position versus time in seconds.

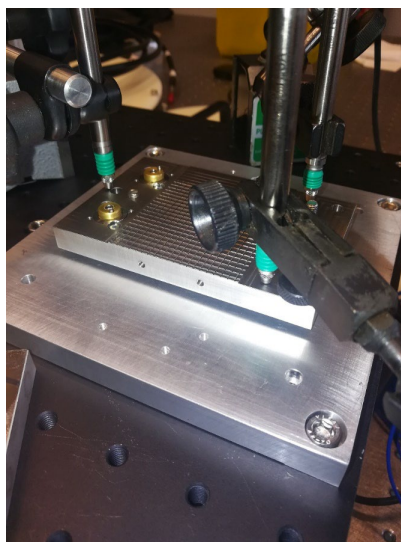


Figure 3-4 : position tuning set up : the differential screws are not visible on the picture.

3.3 Shock resistance

From the same set up, we were also able to run some shock tests. The base plate being fixed to a plate having a controlled Eigen value around 100Hz, we equipped the engineering model with an accelerometer (PCB 352C33) and excited its support with an instrumented test hammer (PCB 086D05). Time signals were recorded using a sound and vibration specific acquisition device (NI-9185/9230), and recorded on a PC. From the recorded file, RMS amplitude signal was computed over a 1 second time, and plotted versus position measurements. Tests were conducted in X, Y and Z directions. Shock intensity was controlled by hand, and increased gradually from few N/mm² up to around 1.5g. Due to the mass of our base plate and the mass of our shock hammer, it was not possible to apply higher forces. One of the results (the one along the z direction) is represented in Figure 3-5. It shows that parasitic movement of the mirror is kept below 1µm and few arcseconds for all shocks.

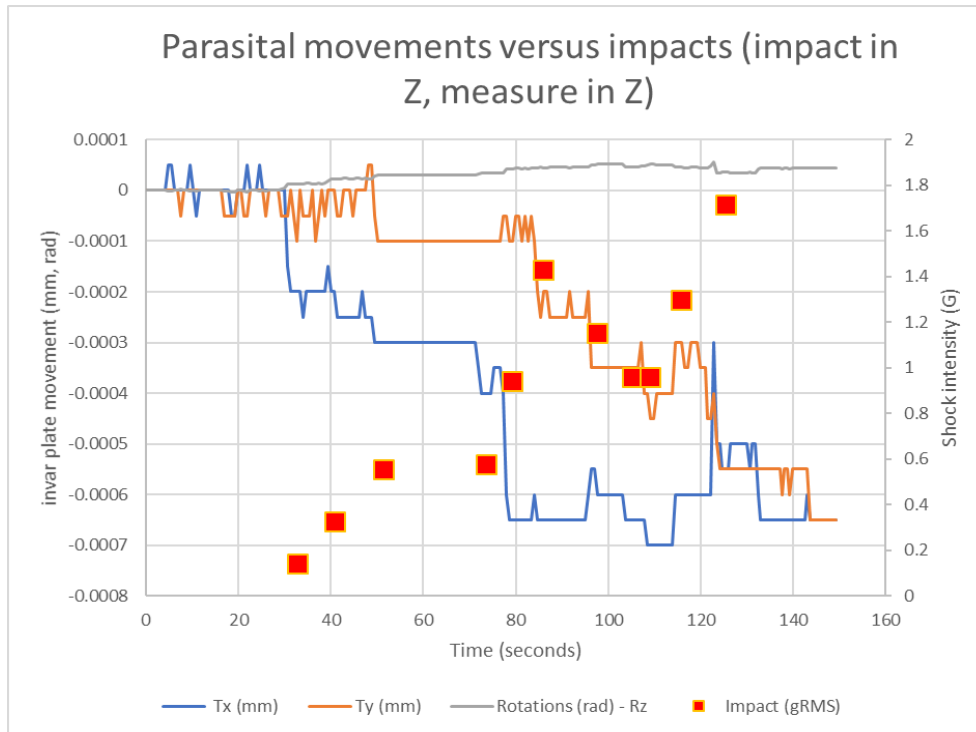


Figure 3-5 : Parasitic movements observed for increasing impacts.

3.4 Position stability during cooling :

While all previous tests were done on the mechanical parts of the prototype, we did not receive the glued mirror yet from its manufacturer. We were not able to conduct these tests with the described prototype in this section at the time of the writing of this article. Nevertheless, tests have been conducted using spherical washers concentric with standard screws, mounted with retaining springs (not differential). The tightening force applied was of the same order of the one foreseen for the differential screws. For this test, our cryostat was equipped with an autocollimator, installed in front of our viewing port, aiming at both the reference mirror and the mirror of the prototype. This set up allows us to have a continuous measurement of the angular position of the mirror during the cooling phase, with a resolution of few arc seconds. The conducted test allows us to see that the spherical washer mounting improves by a factor 3 the stability of our mount, compared to the sphere on plane contact we use with our first prototype. The obtained results are shown in Figure 3-6.

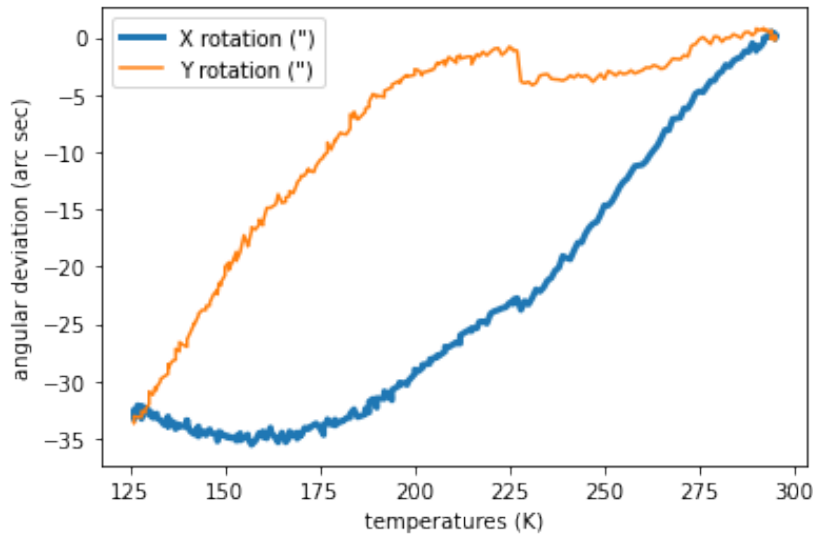


Figure 3-6 : angular stability of spherical washer prototype. The curves show a factor 3 improvement from previous set up.

4. MIRROR MOUNT ALLOWING 6 AXIS POSITION TUNING

4.1 Design description

From the last design, we propose here a last improvement of our setup. This improvement consists of placing the holders of our pistons on a movable stage. This stage is made using classical Electrical Discharge Machining (EDM) in the base plate. The control of the movement is done using 2 special wedges, realizing both the control of the motion and the holding of the motion. Furthermore, this wedge architecture allows us to control the position of our pistons in a direction orthogonal to the desired motion, thus realizing a compact implementation of these functions. Using this architecture, we now have the 6 degrees of freedom of our mirror that can be tuned and blocked. This solution is represented in Figure 4-1.

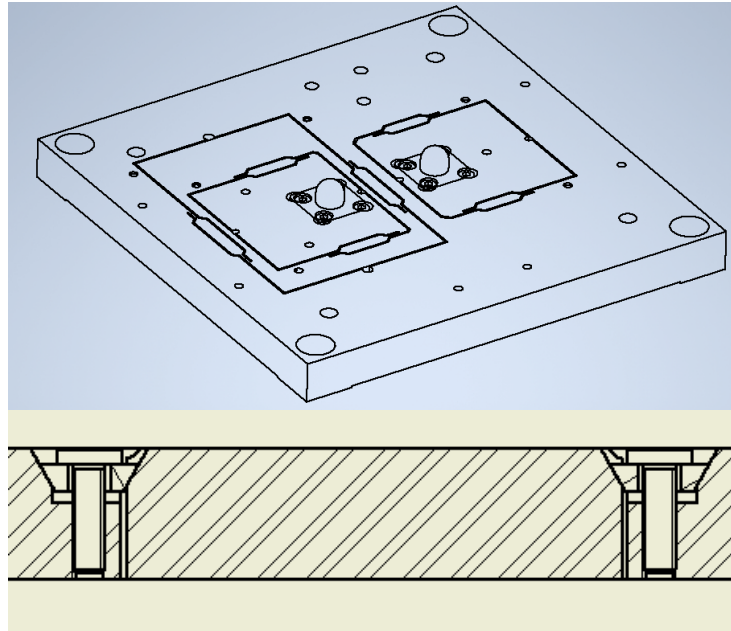


Figure 4-1 : general view of EDM cutting and wedge tuning and blocking functions.

4.2 Tuning resolutions

Here again, we controlled the tuning capabilities of our design in front of numerical gauges. The resolution is only limited by the resolution of our gauges, which is $0.1\mu\text{m}$. The blocking capabilities of our set up were also tested, and similar behavior of the one shown in Figure 3-5 is measured: parasitic movements are limited to $1\mu\text{m}$ and few arcseconds for shocks under 2G.

5. CONCLUSION

In this paper, we have presented a cryogenic mirror mount for the Integral Field Unit of HAMRONI. Due to stringent positioning ($< 10''$) and environmental requirements (cryogenic environment, resistance to earthquakes), these mounts have undergone significant design work over the past months. Our first design, that imposed a full dismounting of the mirror to adjust its position, was compliant in terms of deformation of the optical surface. Nevertheless, its thermal stability was not sufficient, as we measured a significant influence of the thermal braids needed to cool down the mirror. From this design, we proposed a new set up that allows a rapid tuning of the mirror orientation in place on its mounts. The thermal stability was improved to $30''$, removing the thermal braids. In the last section we proposed a last improvement that will allow to tune the six degrees of freedom of the mirror. This set up has not been tested yet, but we are confident that thermal stability and tuning capabilities should be preserved. With these last tests, we should validate our design and allow the IFU to go to its final design review.

The authors are grateful to the LABEX Lyon Institute of Origins (ANR-10-LABX-0066) Lyon for its financial support within the program "Investissements d'Avenir" of the French government operated by the National Research Agency (ANR). This work was also supported by a grant overseen by the French National Research Agency (ANR) as part of the Investments from the Future program, bearing the reference ANR-21-ESRE-0008

REFERENCES

- [1] N. Thatte *et al.*, « HARMONI: first light spectroscopy for the ELT: instrument final design and quantitative performance predictions », in *Ground-based and Airborne Instrumentation for Astronomy VIII*, Online Only, United States, déc. 2020, p. 337. doi: 10.1117/12.2562144.
- [2] N. A. Thatte *et al.*, « The E-ELT first light spectrograph HARMONI: capabilities and modes », Edinburgh, United Kingdom, août 2016, p. 99081X. doi: 10.1117/12.2230629.
- [3] M. Loupias *et al.*, « HARMONI - first light spectroscopy for the ELT: final design of the integral field unit », in *Advances in Optical and Mechanical Technologies for Telescopes and Instrumentation IV*, 2020, vol. 11451, p. 625-635. doi: 10.1117/12.2561374.